

## Controlling magnetic skyrmion nucleation with Ga<sup>+</sup> ion irradiation

Mark C. H. de Jong <sup>\*</sup>, Bennert H. M. Smit , Mariëlle J. Meijer, Juriaan Lucassen ,  
Henk J. M. Swagten , Bert Koopmans, and Reinoud Lavrijsen <sup>†</sup>

*Department of Applied Physics, Eindhoven University of Technology, P.O. Box 513, 5600 MB Eindhoven, the Netherlands*



(Received 23 December 2022; accepted 13 March 2023; published 24 March 2023)

In this paper, we show that magnetic skyrmion nucleation can be controlled using Ga<sup>+</sup> ion irradiation, which manipulates the magnetic interface effects (in particular, the magnetic anisotropy and Dzyaloshinskii-Moriya interaction) that govern the stability and energy cost of skyrmions in thin-film systems. We systematically and quantitatively investigate what effect these changes have on the nucleation of magnetic skyrmions. Our results indicate that the energy cost of skyrmion nucleation can be reduced up to 26% in the studied dose range and that it scales approximately linearly with the square root of the domain wall energy density. Moreover, the total number of nucleated skyrmions in irradiated devices after nucleation was found to depend linearly on the ion dose and could be doubled compared to nonirradiated devices. These results show that ion irradiation cannot only be used to enable local nucleation of skyrmions but also allows for fine control of the threshold and efficiency of the nucleation process.

DOI: [10.1103/PhysRevB.107.094429](https://doi.org/10.1103/PhysRevB.107.094429)

### I. INTRODUCTION

Magnetic skyrmions are a type of chiral magnetic texture that has generated tremendous research interest in recent years [1–5]. Due to their small size down to a few nanometers [5], current-induced motion [6], stability, and topology [7], they are promising candidates for future memory applications [8,9] as well as computing schemes such as neuromorphic computing [10]. Stable skyrmions at room temperature can be readily stabilized and observed in magnetic multilayers, as was shown in Refs. [6,11,12]. A skyrmion in such a system is present in each of the magnetic layers, forming a tube in three dimensions. In a multilayer, skyrmions are stabilized primarily by dipolar interactions which are enhanced due to the large magnetic volume of all the layers combined [13]. A uniform chirality in each layer—which distinguishes skyrmions from magnetic bubbles—is realized by a strong interfacial Dzyaloshinskii-Moriya interaction (DMI) [14,15] which is present and strong in these systems due to the large number of complementary heavy metal/magnet interfaces [12]. Skyrmions can be nucleated in such systems in a variety of ways: using magnetic fields that break larger domains down to skyrmions [16–18], spin-orbit torques at defects [19,20], and thermal fluctuations of the magnetization caused by either ultrafast laser pulses [21,22] or Joule heating during nanosecond current pulses [23,24].

In all the above-mentioned cases, the nucleation of skyrmions occurs at random positions in the material. For many applications, however, it is desirable to be able to nucleate skyrmions at well-defined positions in a device and to control the amount of excitation that is needed to nucleate a skyrmion. Many schemes to achieve this have been experi-

mentally demonstrated or proposed [4,17–20,25–27], but in this paper we focus on the use of Ga<sup>+</sup> ion irradiation.

Ion irradiation can be used to locally tune the magnetic effects originating from interfaces by gradually increasing the degree of intermixing [28–30] in systems consisting of single magnetic layers [18,28–30] and even magnetic multilayers [17,20,31,32]. In the case of field-driven skyrmion nucleation, localized [17,32] as well as nonlocalized [32] Ga<sup>+</sup> ion irradiation has been shown to facilitate field driven skyrmion nucleation. Both studies found that skyrmions nucleate more densely in regions that have been irradiated with Ga<sup>+</sup> ions and were able to nucleate skyrmions at well-defined positions with an applied magnetic field. Recently, there has also been work studying the effect of localized He<sup>+</sup> ion irradiation on the field driven [18] as well as current- and laser-induced nucleation of skyrmions [20] and also their current-driven motion [18,20]. Skyrmion nucleation was achieved exclusively within the irradiated regions of the devices, demonstrating a reduced threshold for nucleation compared to nonirradiated regions. It was also shown that the border between the irradiated and nonirradiated regions presents an energy barrier for skyrmions. However, the cause of the decrease in the nucleation threshold as well as the dependence of the nucleation threshold on the ion dose are still unclear and the extent to which the nucleation threshold can be reduced remains an open question.

We have previously studied the effect that Ga<sup>+</sup> ion irradiation has on the magnetic properties of an [Ir(1)|Co(0.8)|Pt(1)]<sub>×6</sub> multilayer system [31] (all thicknesses in brackets are in nm) and found that the effective anisotropy  $K_{\text{eff}}$  decreases gradually and strongly throughout the tested dose range and that the interfacial DMI strength  $D$  decreases gradually but much less strongly. The effect of these changes is a factor of 2 reduction of the domain-wall energy density,

$$\sigma_{\text{DW}} = 4\sqrt{AK_{\text{eff}}} - \pi|D|, \quad (1)$$

<sup>\*</sup>m.c.h.d.jong@tue.nl

<sup>†</sup>r.lavrijsen@tue.nl

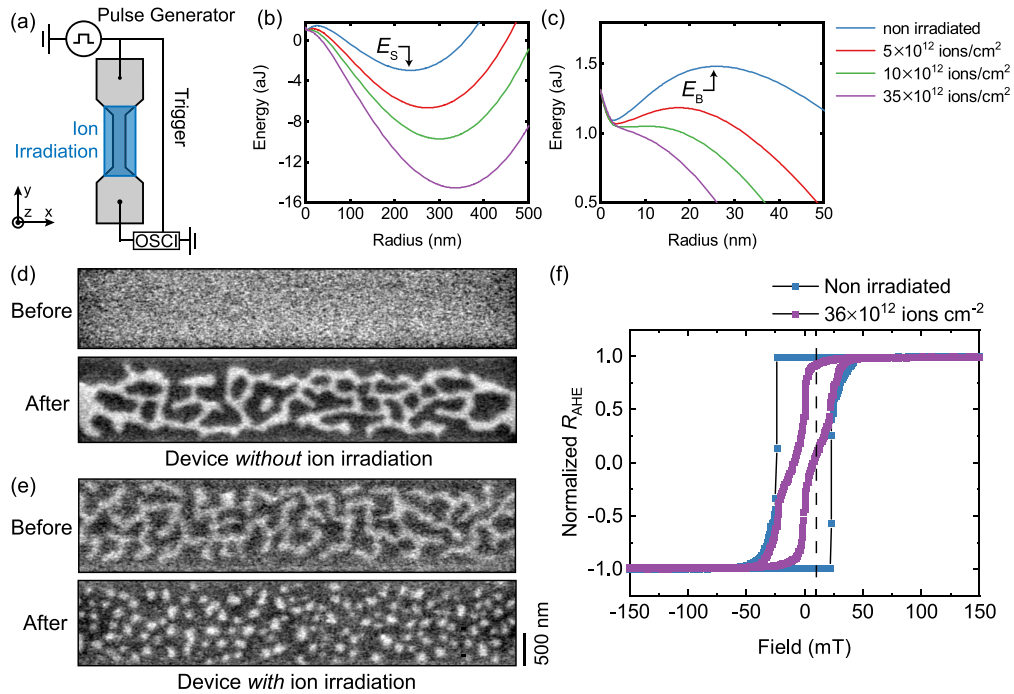


FIG. 1. (a) Schematic overview of the nucleation devices (not to scale). Each device has been irradiated with a different  $\text{Ga}^+$  dose in the region indicated in blue. (b) Energy as a function of skyrmion radius calculated using the model by Büttner *et al.* from Ref. [13] for the magnetic parameters corresponding to different doses of  $\text{Ga}^+$  ion irradiation. (c) Zoom of the energy barrier for skyrmion nucleation. (d) MFM images of the domain state in a nonirradiated device before and after applying a current pulse train with pulses of  $J = 5.54 \times 10^{11} \text{ A m}^2$  in a magnetic field of  $\mu_0 H_z = 10 \text{ mT}$ . (e) MFM images of the magnetic state in a device irradiated with a dose of  $d = 35 \times 10^{12} \text{ ions cm}^{-2}$ . The current density, pulse shape, number of pulses, and magnetic field are all the same as in (d). (f) Hysteresis loops measured in a similar nonirradiated device and a device irradiated with  $d = 36 \times 10^{12} \text{ ions cm}^{-2}$  using the anomalous Hall effect. The dashed line corresponds to the magnetic field applied in (d) and (e). These devices have a thinner Pt(2 nm) buffer layer but are otherwise nominally identical.

where  $A$  is the exchange stiffness. Despite this large decrease, the relatively small decrease in the strength of the DMI ensures that domain walls remain chiral. Hence, we postulated that  $\text{Ga}^+$  ion irradiation would be a convenient tool to manipulate the energy barrier for skyrmions nucleation.

In this paper, we study current-driven nucleation of magnetic skyrmions in the exact same material system as used in Ref. [31] at different  $\text{Ga}^+$  ion doses. By irradiating the entire device, we could study the effect of ion irradiation on the current-driven nucleation of skyrmions in a statistical manner and determine the dependence of the threshold current for skyrmion nucleation and skyrmion density as a function of ion dose. We found that ion irradiation decreases the threshold current for nucleation and that the dependence on the ion dose of the threshold current resembles the dependence of the domain-wall energy density on the ion dose, showing that the change in the magnetic parameters is an important contribution to the modification of the threshold current. Surprisingly, we also found that the skyrmion density in our devices scales linearly with ion dose, doubling in the tested dose range, which enables control of the skyrmion density in devices by ion irradiation.

## II. METHODS

The material stack used throughout this paper is the following magnetic multilayer:  $\text{Si}|\text{SiO}_2(100)|\text{Ta}(4)|\text{Pt}(15)|[\text{Ir}(1)|\text{Co}(0.8)|\text{Pt}(1)]_{\times 6}|\text{Pt}(2)$ . All layers were grown using DC

magnetron sputtering in an argon atmosphere with partial pressure of  $2 \times 10^{-3} \text{ mbar}$ . The system had a base pressure of  $\sim 5 \times 10^{-9} \text{ mbar}$ . The nucleation devices were patterned using electron beam lithography in combination with liftoff and consist of a  $7\text{-}\mu\text{m}$ -long and  $1.5\text{-}\mu\text{m}$ -wide strip [see Fig. 1(a)].  $\text{Ga}^+$  ion irradiation of this strip was performed using the  $\text{Ga}^+$  focused ion beam in a FEI Nova NanoLab Dualbeam, with an acceleration voltage of 30 keV and a beam current of approximately 1.5 pA. To irradiate areas larger than the beam diameter, the beam was rasterscanned across the sample. The dose  $d$  was calculated as

$$d = \frac{\text{BC} \times \text{DT}}{\text{LS} \times \text{SS}}, \quad (2)$$

where BC is the beam current, DT is the dwell time at each position, and LS and SS are the line and spot spacing, respectively. The line and spot spacing were limited by the minimum dwell time and maximum beam speed and were set to 80 nm for all devices used in this paper. It is likely that the spot size of the ion beam was smaller than the spot and line spacing during irradiation, since at optimal focus the system has a resolution of approximately 20 nm [33]. Nevertheless, the spot and line spacing is smaller than all skyrmions that were observed and no obvious square pattern is present in the nucleation sites (see Supplemental Material S4 [34]; see, also, Refs. [13,35,36] therein).

The fabricated and irradiated devices were mounted in a custom sample holder positioned in a Bruker Dimension

Edge atomic force microscope that was used for magnetic force microscopy (MFM) measurements using custom coated low moment tips [Ta(4)|Co(7.5)|Ta(5) sputter deposited onto Nanosensors PPP-FMR tips]. The sample holder enables manipulation of the magnetic state of the multilayers using nanosecond current pulses as well as the simultaneous application of a magnetic field up to  $\mu_0 H_z = 500$  mT during measurements. Skyrmion nucleation was achieved by sending bipolar pulse trains of nanosecond current pulses using an Agilent 33250A 80 MHz arbitrary waveform generator. The pulses were measured using an Agilent Infiniium DSO80604B oscilloscope connected in series with the nucleation devices. The current through the device was calculated by dividing the pulse voltage as measured with the oscilloscope by the resistance of the oscilloscope ( $50 \Omega$ ). The current density was calculated by assuming that the current is uniformly distributed throughout the entire multilayer stack.

### III. RESULTS AND DISCUSSION

To motivate why the nucleation of skyrmions should be affected by a decrease in the domain-wall energy density, we consider a model of the skyrmion energy from Ref. [13]. In Figs. 1(b) and 1(c), we plot the energy of a skyrmion as a function of its radius for the structural and magnetic parameters measured for our (irradiated) Ir|Co|Pt multilayer system in Ref. [31]. For increasing ion dose, we indeed observe that the local energy maximum  $E_B$  [Fig. 1(c)] that prevents nucleation of a skyrmion, and is related to the competition between the domain-wall energy (and the Zeeman energy) with the dipolar energy, decreases in magnitude. Although this model of a nucleation process is likely oversimplified, we still expect a decrease in the domain-wall energy density to affect the nucleation since this always includes an increase in the domain wall length. The model also predicts a decrease in the energy minimum  $E_S$  [Fig. 1(b)], which means that the energy of a skyrmion is lower in an irradiated part of the sample than a nonirradiated part. This matches the observation in Ref. [18] that the border between these regions represents an energy barrier for a skyrmion. These results suggest that  $\text{Ga}^+$  ion irradiation should indeed affect the nucleation of magnetic skyrmions.

To experimentally study the dependence of the current driven skyrmion nucleation on the  $\text{Ga}^+$  dose, we utilized devices shown schematically in Fig. 1(a). First, the magnetization in the device was saturated by applying a magnetic field of  $\mu_0 H_z = -150$  mT. Next, a small bias field  $\mu_0 H_z = 10$  mT with the opposite polarity was applied for the duration of the measurement. To nucleate skyrmions, we applied a pulse train consisting of 1000 bipolar nanosecond current pulses with a current density in the order of  $10^{11}$  A/m<sup>2</sup> (pulse length: 50 ns, time between pulses: 1  $\mu$ s). This is a similar nucleation scheme as used in Refs. [23,24], where the nucleation is primarily driven by Joule heating. This increase in temperature drives fluctuations in the magnetization that result in the formation of topological charge and hence skyrmions [24]. We used this method of nucleation because the relative change in Joule heating required for skyrmion nucleation can be easily determined by measuring the threshold current density for

nucleation and the resistance of the devices as a function of ion dose.

Two examples that show that  $\text{Ga}^+$  ion irradiation indeed had a large effect on the nucleation of skyrmions are shown in Figs. 1(d) and 1(e). In Fig. 1(d), we show MFM images of the magnetic domain state in a nonirradiated device before and after applying a pulse train with a current density of  $J = 5.54 \times 10^{11}$  A m<sup>2</sup> (bias field parallel to the dark domain). Only one skyrmion was present in the device after applying the pulses. However, when we applied the same pulse train and magnetic field to a device that had been irradiated with  $d = 35 \times 10^{12}$  ions cm<sup>-2</sup>, we found that the device was in a state where only skyrmions remained [Fig. 1(e)]. We also show two anomalous Hall effect measurements that were done as a function of magnetic field in two similar devices in Fig. 1(f) to illustrate the effect of the ion irradiation on the magnetic hysteresis loops. The loop changed from a square loop in the nonirradiated device to a slanted loop in the irradiated device. In the remainder of this paper, we study the effect on nucleation in more detail and examine how strongly the nucleation of skyrmions can be controlled.

To do this, we require a measure for the energy required to nucleate skyrmions in our devices. The threshold current density is a logical choice but the transition between states with no skyrmions and only skyrmions is not infinitely sharp and therefore it is not enough to only look at whether one or more skyrmions is present in the device. Hence, we measured the number of skyrmions in the device after applying a train of current pulses as a function of current density. All measurements were performed with the same bias field of  $\mu_0 H_z = 10$  mT (in the Supplemental Material SII, we show that skyrmions were nucleated in both nonirradiated devices and irradiated devices for this bias field.) To obtain the amount of nucleated skyrmions, we used a MatLab script which is based on a skyrmion counting procedure described in Ref. [36] and is described in the Supplemental Material SIII. For each current density, three nucleation events were observed and the number of skyrmions was averaged. As a measure for the uncertainty in the final number of skyrmions, we took the standard deviation of this average.

The results for a nonirradiated device are shown in Fig. 2(a) where the number of skyrmions is plotted as a function of current density. For low current densities ( $J < 5 \times 10^{11}$  A m<sup>-2</sup>), the effect on the magnetization was not strong enough to nucleate skyrmions and no skyrmions appear in the device [Fig. 2(b)]. For high current densities ( $J > 6 \times 10^{11}$  A m<sup>-2</sup>), on average 40 skyrmions were nucleated in the device [Fig. 2(d)]. In between, a sharp transition was found where a threshold current for nucleation is exceeded. To determine this threshold current accurately we fit the data with the following phenomenological model:

$$N_{\text{sk}} = \frac{1}{2} N_{\text{sk,sat}} \left( 1 + \text{erf} \left( \frac{J - J_c}{\sqrt{2} \Delta} \right) \right), \quad (3)$$

where  $J_c$  is the threshold current,  $N_{\text{sk}}$  ( $N_{\text{sk,sat}}$ ) is the number of skyrmions (above the threshold current),  $\Delta$  is the width of the transition region and  $\text{erf}()$  is the error function. The threshold current is found to be  $J_c = (5.68 \pm 0.02) \times 10^{11}$  A m<sup>-2</sup> for the nonirradiated device, where we have taken the fit

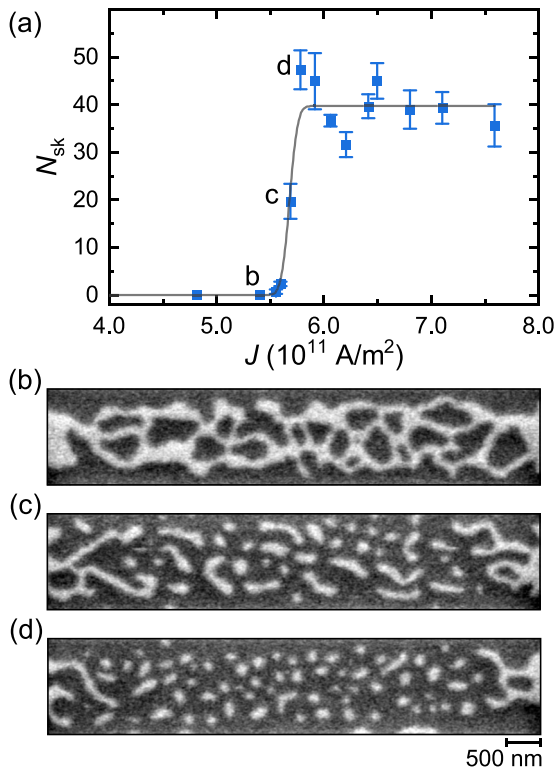


FIG. 2. (a) The number of skyrmions that appear in a device after applying a sequence of 1000 bipolar current pulses with a length of 50 ns and a time between pulses of 1  $\mu\text{s}$  plotted as a function of the applied current density. Each measurement point is an average of three nucleation events; error bars represent one standard deviation. The gray line is a fit to the data with the error function, Eq. (3). (b)–(d) MFM images of the magnetization state in the device after applying the pulses, the corresponding current densities have been labeled in (a). Dark contrast is parallel to the applied bias field.

uncertainty as the error in the threshold current. Additionally, we can now conclude that the width of the transition region  $\Delta = (0.06 \pm 0.02) \times 10^{11} \text{ A m}^{-2}$  is much less than the threshold current, i.e., the transition is sharp. Now that we have established a method to reliably determine the threshold current needed for the nucleation of skyrmions, we can look at the effect of ion irradiation on the threshold current.

The experiment highlighted in Fig. 2(a) was repeated for several ion doses up to  $d = 35 \times 10^{12} \text{ Ga}^+ \text{ ions cm}^{-2}$ . The results are plotted in Fig. 3(a) for six different ion doses between zero and  $d = 35 \times 10^{12} \text{ ions cm}^{-2}$ . Each data set is fitted with Eq. (3), which is in good agreement with the data for all doses. We begin by examining the change in the threshold current  $J_c$  as a function of ion dose. In Fig. 3(a), the two dotted lines represent the threshold current for the nonirradiated device (blue squares) and the device with the highest ion dose (brown triangles pointing left). It is apparent that the ion irradiation has significantly lowered the threshold current required for skyrmion nucleation. To determine the dependence in more detail, we have plotted the threshold current against the  $\text{Ga}^+$  ion dose in Fig. 3(b). For doses up to  $d = 15 \times 10^{12} \text{ ions cm}^{-2}$ , the threshold current reduces monotonously as a function of dose. At this dose, the decrease stops and for larger doses the threshold current appears to

saturate at a value of  $J_c = (4.92 \pm 0.06) \times 10^{11} \text{ A m}^{-2}$ . This trend is similar to the trend we observed for the domain-wall energy density as a function of ion dose [31]. In the Supplemental Material SI, we also show that the observed change in the threshold current is much larger than the naturally occurring variation in threshold current between devices, indicating that the observed reduction in threshold current is a result of the ion irradiation.

We assume that a thermal mechanism (as in Refs. [23,24]) is also the dominant mechanism for nucleation in the system used here. Evidence for this is the observation that the required current density for nucleation decreased when the pulse length was increased [compare Fig. S2(a) in the Supplemental Material with 10 ns pulses to Fig. 2(a) with 50 ns pulses]. This is expected for thermally driven nucleation but not for SOT-driven nucleation, since this should happen at timescales on the order of 1 ns [24]. With this assumption, the energy that is deposited into the system scales with  $J^2$ . Hence, the relative difference in energy requirement for the nonirradiated device and the device irradiated with  $d = 35 \times 10^{12} \text{ ions cm}^{-2}$  can be calculated as  $(J_{c,d=0}^2 - J_{c,d=35}^2)/J_{c,d=0}^2 = 0.26$ , i.e., the energy required for nucleating skyrmions is reduced by 26%<sup>1</sup>.

In the inset of Fig. 3(b), we have also plotted the measured threshold current squared as a function of the measured domain-wall energy density at room temperature from Ref. [31]. We find that for doses up to  $d = 15 \times 10^{12} \text{ ions cm}^{-2}$ , there is an approximately linear dependence of  $J_c^2$  on  $\sigma_{\text{DW,RT}}$  as expected when Joule heating is the dominant mechanism for nucleation. However, the range of domain-wall energies that we were able to probe with ion irradiation was too small to conclusively determine the relation between the critical current and the domain wall energy density.

A second observation is that the number of skyrmions that appeared in the bar for current densities larger than the threshold current increased with increasing ion dose. This behavior is clear when we plot the number of skyrmions at saturation  $N_{sk,\text{sat}}$  as a function of the ion dose in Fig. 3(c). In the nonirradiated device, there was an average of 40 skyrmions in the device after applying a sufficiently strong current pulse train. This number increased linearly with ion dose to 80 skyrmions for the device with  $d = 35 \times 10^{12} \text{ ions cm}^{-2}$ , a doubling of the total number of skyrmions. An increase of the skyrmion density with increasing  $\text{Ga}^+$  ion dose has also been observed in field-driven nucleation experiments [32] and is expected when reducing the domain-wall energy density [16]. Considering that the decrease in the domain-wall energy density as a function of dose in our samples slows down for doses larger than  $d = 15 \times 10^{12} \text{ ions cm}^{-2}$  [31], a linear increase in the number of skyrmions cannot be explained by a decrease in the domain-wall energy alone, which could suggest that the number of nucleation sites in the device also increases as a function of  $\text{Ga}^+$  ion dose.

One final observation we can make from Fig. 3(a) is that for higher ion doses, the width of the transition region between

<sup>1</sup>The resistance increases slightly with ion dose as well, but is only 4% higher in the device irradiated with  $d = 35 \times 10^{12} \text{ ions cm}^{-2}$  compared to the nonirradiated device and hence this is not enough to explain the decrease in the required Joule heating for nucleation.

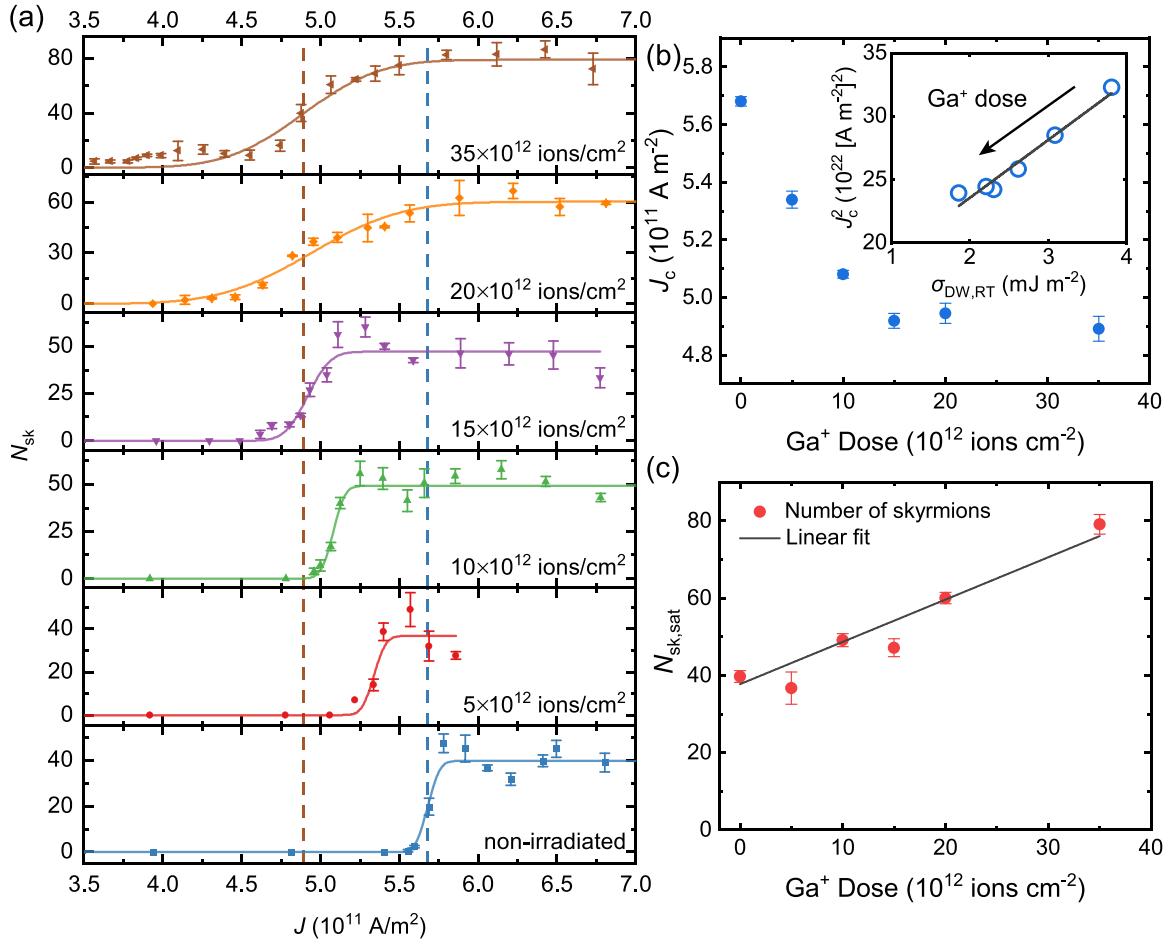


FIG. 3. (a) The number of skyrmions in a device after applying a sequence of 1000 bipolar current pulses plotted as a function of the applied current density for several devices irradiated with different Ga<sup>+</sup> doses. The lines are fits to the data with the error function, Eq. (3). (b) The threshold current  $J_c$ , extracted from the data in (a), plotted as a function of the Ga<sup>+</sup> dose. Inset: The threshold current squared plotted as a function of the domain-wall energy density  $\sigma_{DW,RT}$ , measured for the same material system at room temperature in Ref. [31]. The dark grey line is a linear fit to the data. (c) Average number of skyrmions that appear in the device for current densities larger than the threshold current plotted as a function of Ga<sup>+</sup> dose. The dark grey line is a linear fit to the data.

no skyrmions and saturation increased significantly. The good agreement between the data and Eq. (3) for all doses indicates that the nucleation current followed a normal distribution with  $\Delta$  the standard deviation, which broadens significantly for doses above  $d = 15 \times 10^{12}$  ions cm<sup>-2</sup>. At this dose, we also observed that the domain-wall energy stops decreasing as a function of ion dose and saturated [31]. This suggests that at higher doses, the variance in the magnetic parameters might be more strongly affected by ion irradiation than the average value, i.e., the local variation of magnetic interface effects in the material increases. This hypothesis is also in line with an increase in the number of nucleation sites as postulated in the previous paragraph. However, verifying this hypothesis by measuring the magnitude of such local variations in the magnetic interface parameters as a function of ion dose is beyond the scope of this paper.

#### IV. CONCLUSION AND OUTLOOK

In this paper, we have reported the effect of Ga<sup>+</sup> ion irradiation on the current-driven nucleation of skyrmions

in a magnetic multilayer. We uniformly irradiated our devices, which enabled us to study the effect that changes in the magnetic parameters due to the irradiation have on the current-driven nucleation process, contrary to earlier work where the authors primarily looked at nucleation from small irradiated regions [17,18,20]. We found that the threshold current for skyrmion nucleation can be reduced for Ga<sup>+</sup> doses up to  $d = 15 \times 10^{12}$  ions cm<sup>-2</sup> and that for larger doses the threshold current saturates. Additionally, and perhaps more importantly for applications where precise control of the skyrmion nucleation sites is desired, for doses up to  $d = 15 \times 10^{12}$  ions cm<sup>-2</sup> there exists a current density where the number of skyrmions is maximized in the irradiated device while no skyrmions are formed in the nonirradiated device for the same current density. This enables the localization of current [20] and field [18,32] driven skyrmion nucleation in devices. Surprisingly, this is not the case for the largest two doses studied, which suggest that there exists an optimal Ga<sup>+</sup> dose for the localization which should depend on the material stack and the parameters of the ion beam.

The number of skyrmions that can be nucleated in a device was found to depend linearly on the ion dose. Contrary to the threshold current, the number of skyrmions keeps increasing for the entire dose range. This observation might be interesting for multistate memory applications [37,38] as well as neuromorphic computation applications [10,39], since this means that the average number of skyrmions after nucleation in a device can be effectively controlled using  $\text{Ga}^+$  ion irradiation. Furthermore, by utilizing the ability to pattern the ion irradiation, it would be possible to control the skyrmion density in devices locally, a hitherto unexplored possibility in skyrmion devices. Finally, we showed that the distribution of nucleation currents becomes broader for devices irradiated with a relatively large ion dose. This could be useful in applications where a more precise control of the skyrmion number is required than can be provided by nonirradiated

material systems. Concluding, we have shown that  $\text{Ga}^+$  ion irradiation can be used to effectively control the threshold current and efficiency of the current-driven nucleation of magnetic skyrmions.

#### ACKNOWLEDGMENTS

This work is part of the Gravitation programme Research Centre for Integrated Nanophotonics, which is financed by the Dutch Research Council (NWO). M.J.M. and J.L. acknowledge support as part of the research program of the Foundation for Fundamental Research on Matter (FOM), which is a part of NWO. This work was supported by the Eindhoven Hendrik Casimir Institute.

M.C.H.J. and B.H.M.S. contributed equally.

- 
- [1] R. Wiesendanger, Nanoscale magnetic skyrmions in metallic films and multilayers: A new twist for spintronics, *Nat. Rev. Mater.* **1**, 16044 (2016).
- [2] A. Fert, N. Reyren, and V. Cros, Magnetic skyrmions: Advances in physics and potential applications, *Nat. Rev. Mater.* **2**, 17031 (2017).
- [3] K. Everschor-Sitte, J. Masell, R. M. Reeve, and M. Kläui, Perspective: Magnetic skyrmions—Overview of recent progress in an active research field, *J. Appl. Phys.* **124**, 240901 (2018).
- [4] X. Zhang, Y. Zhou, K. M. Song, T.-E. Park, J. Xia, M. Ezawa, X. Liu, W. Zhao, G. Zhao, and S. Woo, Skyrmion-electronics: Writing, deleting, reading and processing magnetic skyrmions toward spintronic applications, *J. Phys.: Condens. Matter* **32**, 143001 (2020).
- [5] Y. Tokura and N. Kanazawa, Magnetic skyrmion materials, *Chem. Rev.* **121**, 2857 (2021).
- [6] S. Woo, K. Litzius, B. Krüger, M.-Y. Im, L. Caretta, K. Richter, M. Mann, A. Krone, R. M. Reeve, M. Weigand, P. Agrawal, I. Lemesh, M.-A. Mawass, P. Fischer, M. Kläui, and G. S. D. Beach, Observation of room-temperature magnetic skyrmions and their current-driven dynamics in ultrathin metallic ferromagnets, *Nat. Mater.* **15**, 501 (2016).
- [7] S.-G. Je, H.-S. Han, S. K. Kim, S. A. Montoya, W. Chao, I.-S. Hong, E. E. Fullerton, K.-S. Lee, K.-J. Lee, M.-Y. Im, and J.-I. Hong, Direct demonstration of topological stability of magnetic skyrmions via topology manipulation, *ACS Nano* **14**, 3251 (2020).
- [8] R. Tomasello, E. Martinez, R. Zivieri, L. Torres, M. Carpentieri, and G. Finocchio, A strategy for the design of skyrmion race-track memories, *Sci. Rep.* **4**, 6784 (2014).
- [9] S. Luo and L. You, Skyrmion devices for memory and logic applications, *APL Mater.* **9**, 050901 (2021).
- [10] J. Grollier, D. Querlioz, K. Y. Camsari, K. Everschor-Sitte, S. Fukami, and M. D. Stiles, Neuromorphic spintronics, *Nat. Electron.* **3**, 360 (2020).
- [11] O. Boulle, J. Vogel, H. Yang, S. Pizzini, D. de Souza Chaves, A. Locatelli, T. O. Mentes, A. Sala, L. D. Buda-Prejbeanu, O. Klein, M. Belmeguenai, Y. Roussigné, A. Stashkevich, S. M. Chérif, L. Aballe, M. Foerster, M. Chshiev, S. Auffret, I. M. Miron, and G. Gaudin, Room-temperature chiral magnetic skyrmions in ultrathin magnetic nanostructures, *Nat. Nanotechnol.* **11**, 449 (2016).
- [12] C. Moreau-Luchaire, C. Moutafis, N. Reyren, J. Sampaio, C. A. F. Vaz, N. Van Horne, K. Bouzehouane, K. Garcia, C. Deranlot, P. Warnicke, P. Wohlhüter, J.-M. George, M. Weigand, J. Raabe, V. Cros, and A. Fert, Additive interfacial chiral interaction in multilayers for stabilization of small individual skyrmions at room temperature, *Nat. Nanotechnol.* **11**, 444 (2016).
- [13] F. Büttner, I. Lemesh, and G. S. D. Beach, Theory of isolated magnetic skyrmions: From fundamentals to room temperature applications, *Sci. Rep.* **8**, 4464 (2018).
- [14] I. Dzyaloshinsky, A thermodynamic theory of “weak” ferromagnetism of antiferromagnetics, *J. Phys. Chem. Solids* **4**, 241 (1958).
- [15] T. Moriya, Anisotropic superexchange interaction and weak ferromagnetism, *Phys. Rev.* **120**, 91 (1960).
- [16] A. Soumyanarayanan, M. Raju, A. L. Gonzalez Oyarce, A. K. C. Tan, M.-Y. Im, A. P. Petrović, P. Ho, K. H. Khoo, M. Tran, C. K. Gan, F. Ernult, and C. Panagopoulos, Tunable room-temperature magnetic skyrmions in Ir/Fe/Co/Pt multilayers, *Nat. Mater.* **16**, 898 (2017).
- [17] K. Fallon, S. Hughes, K. Zeissler, W. Legrand, F. Ajejas, D. Maccariello, S. McFadzean, W. Smith, D. McGrouther, S. Collin, N. Reyren, V. Cros, C. H. Marrows, and S. McVitie, Controlled individual skyrmion nucleation at artificial defects formed by ion irradiation, *Small* **16**, 1907450 (2020).
- [18] R. Juge, K. Bairagi, K. G. Rana, J. Vogel, M. Sall, D. Mailly, V. T. Pham, Q. Zhang, N. Sisodia, M. Foerster, L. Aballe, M. Belmeguenai, Y. Roussigné, S. Auffret, L. D. Buda-Prejbeanu, G. Gaudin, D. Ravelosona, and O. Boulle, Helium ions put magnetic skyrmions on the track, *Nano Lett.* **21**, 2989 (2021).
- [19] F. Büttner, I. Lemesh, M. Schneider, B. Pfau, C. M. Günther, P. Hessing, J. Geilhufe, L. Caretta, D. Engel, B. Krüger, J. Viehhaus, S. Eisebitt, and G. S. D. Beach, Field-free deterministic ultrafast creation of magnetic skyrmions by spin-orbit torques, *Nat. Nanotechnol.* **12**, 1040 (2017).
- [20] L.-M. Kern, B. Pfau, V. Deinhart, M. Schneider, C. Klose, K. Gerlinger, S. Wittrock, D. Engel, I. Will, C. M. Günther, R. Liefferink, J. H. Mentink, S. Wintz, M. Weigand, M.-J.

- Huang, R. Battistelli, D. Metternich, F. Büttner, K. Höflich, and S. Eisebitt, Deterministic generation and guided motion of magnetic skyrmions by focused He<sup>+</sup>-ion irradiation, *Nano Lett.* **22**, 4028 (2022).
- [21] S.-G. Je, P. Vallobra, T. Srivastava, J.-C. Rojas-Sánchez, T. H. Pham, M. Hehn, G. Malinowski, C. Baraduc, S. Auffret, G. Gaudin, S. Mangin, H. Béa, and O. Boulle, Creation of magnetic skyrmion bubble lattices by ultrafast laser in ultrathin films, *Nano Lett.* **18**, 7362 (2018).
- [22] F. Büttner, B. Pfau, M. Böttcher, M. Schneider, G. Mercurio, C. M. Günther, P. Hessing, C. Klose, A. Wittmann, K. Gerlinger, L.-M. Kern, C. Strüber, C. von Korff Schmising, J. Fuchs, D. Engel, A. Churikova, S. Huang, D. Suzuki, I. Lemesch, M. Huang *et al.*, Observation of fluctuation-mediated picosecond nucleation of a topological phase, *Nat. Mater.* **20**, 30 (2021).
- [23] W. Legrand, D. Maccariello, N. Reyren, K. Garcia, C. Moutafis, C. Moreau-Luchaire, S. Collin, K. Bouzehouane, V. Cros, and A. Fert, Room-temperature current-induced generation and motion of sub-100 nm skyrmions, *Nano Lett.* **17**, 2703 (2017).
- [24] I. Lemesch, K. Litzius, M. Böttcher, P. Bassirian, N. Kerber, D. Heinze, J. Zázvorka, F. Büttner, L. Caretta, M. Mann, M. Weigand, S. Finizio, J. Raabe, M.-Y. Im, H. Stoll, G. Schütz, B. Dupé, M. Kläui, and G. S. D. Beach, Current induced skyrmion generation through morphological thermal transitions in chiral ferromagnetic heterostructures, *Adv. Mater.* **30**, 1805461 (2018).
- [25] S. Finizio, K. Zeissler, S. Wintz, S. Mayr, T. Weßels, A. J. Huxtable, G. Burnell, C. H. Marrows, and J. Raabe, Deterministic field-free skyrmion nucleation at a nanoengineered injector device, *Nano Lett.* **19**, 7246 (2019).
- [26] K. Ohara, X. Zhang, Y. Chen, Z. Wei, Y. Ma, J. Xia, Y. Zhou, and X. Liu, Confinement and protection of skyrmions by patterns of modified magnetic properties, *Nano Lett.* **21**, 4320 (2021).
- [27] K. Everschor-Sitte, M. Sitte, T. Valet, A. Abanov, and J. Sinova, Skyrmion production on demand by homogeneous DC currents, *New J. Phys.* **19**, 092001 (2017).
- [28] T. Devolder, Light ion irradiation of Co/Pt systems: Structural origin of the decrease in magnetic anisotropy, *Phys. Rev. B* **62**, 5794 (2000).
- [29] R. Hyndman, P. Warin, J. Gierak, J. Ferré, J. N. Chapman, J. P. Jamet, V. Mathet, and C. Chappert, Modification of Co/Pt multilayers by gallium irradiation—Part 1: The effect on structural and magnetic properties, *J. Appl. Phys.* **90**, 3843 (2001).
- [30] C. Vieu, J. Gierak, H. Launois, T. Aign, P. Meyer, J. P. Jamet, J. Ferré, C. Chappert, T. Devolder, V. Mathet, and H. Bernas, Modifications of magnetic properties of Pt/Co/Pt thin layers by focused gallium ion beam irradiation, *J. Appl. Phys.* **91**, 3103 (2002).
- [31] M. C. H. de Jong, M. J. Meijer, J. Lucassen, J. van Liempt, H. J. M. Swagten, B. Koopmans, and R. Lavrijsen, Local control of magnetic interface effects in chiral Ir|Co|Pt multilayers using Ga<sup>+</sup> ion irradiation, *Phys. Rev. B* **105**, 064429 (2022).
- [32] Y. Hu, S. Zhang, Y. Zhu, C. Song, J. Huang, C. Liu, X. Meng, X. Deng, L. Zhu, C. Guan, H. Yang, M. Si, J. Zhang, and Y. Peng, Precise tuning of skyrmion density in a controllable manner by ion irradiation, *ACS Appl. Mater. Interfaces* **14**, 34011 (2022).
- [33] J. H. Franken, M. Hoeijmakers, R. Lavrijsen, J. T. Kohlhepp, H. J. M. Swagten, B. Koopmans, E. van Veldhoven, and D. J. Maas, Precise control of domain wall injection and pinning using helium and gallium focused ion beams, *J. Appl. Phys.* **109**, 07D504 (2011).
- [34] See Supplemental Material at <https://link.aps.org/supplemental/10.1103/PhysRevB.107.094429> for (1) measurements in a nominally identical device at zero dose, (2) skyrmion nucleation as a function of both applied magnetic field and current, (3) an overview of the skyrmion counting script, and (4) an overview of the MFM scans used in Fig. 3(a). It additionally includes Refs. [13,35,36].
- [35] A. Fernández Scarioni, C. Barton, H. Corte-León, S. Sievers, X. Hu, F. Ajejas, W. Legrand, N. Reyren, V. Cros, O. Kazakova, and H. W. Schumacher, Thermoelectric Signature of Individual Skyrmions, *Phys. Rev. Lett.* **126**, 077202 (2021).
- [36] A. K. C. Tan, J. Lourembam, X. Chen, P. Ho, H. K. Tan, and A. Soumyanarayanan, Skyrmion generation from irreversible fission of stripes in chiral multilayer films, *Phys. Rev. Mater.* **4**, 114419 (2020).
- [37] X. Zhang, W. Cai, X. Zhang, Z. Wang, Z. Li, Y. Zhang, K. Cao, N. Lei, W. Kang, Y. Zhang, H. Yu, Y. Zhou, and W. Zhao, Skyrmions in magnetic tunnel junctions, *ACS Appl. Mater. Interfaces* **10**, 16887 (2018).
- [38] S. Li, A. Du, Y. Wang, X. Wang, X. Zhang, H. Cheng, W. Cai, S. Lu, K. Cao, B. Pan, N. Lei, W. Kang, J. Liu, A. Fert, Z. Hou, and W. Zhao, Experimental demonstration of skyrmionic magnetic tunnel junction at room temperature, *Sci. Bull.* **67**, 691 (2022).
- [39] D. Pinna, G. Bourianoff, and K. Everschor-Sitte, Reservoir Computing with Random Skyrmion Textures, *Phys. Rev. Appl.* **14**, 054020 (2020).